PROCEEDINGS OF
INTERNATIONAL CONFERENCE ON NEW TRENDS IN APPLIED SCIENCES
https://proceedings.icontas.org/
International Conference on New Trends in Applied Sciences (ICONTAS'23), Konya, December 1-3, 2023.

Numerical Investigation of Thermoelectric Generator for Waste Heat Recovery of Diesel Engine

Mahdi Asadi
Department of Energy Systems Engineering, School of Advanced Technologies, Iran University of Science and Technology, Tehran, Iran, ORCID 0000-0002-9702-1873
ma_asadi@alumni.iust.ac.ir

Amir Musa Abazari[*]
Department of Mechanical Engineering, Faculty of Engineering, Urmia University, Urmia, Iran, ORCID 0000-0003-4987-203X
am.abazari@urmia.ac.ir

Iman Larki
Department of Energy Systems Engineering, School of Advanced Technologies, Iran University of Science and Technology, Tehran, Iran, ORCID 0000-0002-1658-1984
iman_larki@nt.iust.ac.ir

ABSTRACT: Thermoelectric generators hold immense promise in addressing the ever-increasing global energy demands and environmental concerns. Harnessing waste heat from various sources, such as exhaust gases from internal combustion engines, represents a vital avenue for improving energy efficiency and reducing emissions. In light of this, the present study introduces a comprehensive model for evaluating the performance of thermoelectric generators in heat recovery from diesel engine exhaust, shedding light on the potential of this technology to contribute to sustainable energy solutions. In this study, a model is presented for evaluating a thermoelectric generator's performance in heat recovery. The model is validated using experimental data from the literature. In this setup, 14 thermoelectric modules are placed at both the bottom and top of a rectangular gas channel of a diesel engine to recover heat from the exhaust gas. The hot head is heated by the exhaust gas, while the cold head is cooled by water, maintaining a constant temperature of 293 K. However, the temperature of the hot head varies depending on the engine's speed and load. The study investigates 12 different engine operating modes, including three motor speed modes (1000, 1500, and 2000 rpm) and five motor load modes (0.2, 0.4, 0.6, 0.8, and 1.0 MPa). Numerical analysis is performed concurrently with finite element simulations. The numerical and experimental finite element results are compared, and the findings confirm the consistency of the results.

Key words: Thermoelectric, Heat Recovery, Energy Harvesting, Diesel Engine, Energy Conversion

INTRODUCTION

The increase in population and the ongoing urbanization process are propelling the need for more energy (Asadi, Larki, et al., 2023). Even though renewable energy technologies have advanced, the majority of this energy demand is still satisfied through the use of fossil fuels (Asadi, Ahmadi, et al., 2023; Larki et al., 2023). In today's world, where we are all striving for cleaner energy and sustainability, there is a smart way to make use of the heat that is typically wasted by diesel engines. These engines are powerful but not very efficient, and a lot of the energy they produce just goes to waste in the form of heat. Thermoelectric generators have a simple but brilliant idea: they can turn that wasted heat into electricity. In other words, they can help make diesel engines more eco-friendly while getting more energy out of them. Thermoelectrics are materials that have the unique ability to convert heat into electricity and vice versa through a phenomenon called the Seebeck effect.

The Seebeck effect, also known as the thermoelectric effect, is a fundamental phenomenon that underlies the operation of thermoelectric materials and devices. It was discovered by the German physicist Thomas Johann

---

[*] Corresponding Author.

Seebeck in the early 19th century. The key principle of the Seebeck effect is that it relates to the generation of an electric voltage (or electromotive force, EMF) when there is a temperature difference between two junctions of dissimilar materials. In other words, it is a direct conversion of a thermal gradient (temperature difference) into electrical voltage. This effect is the basis for the operation of thermocouples, which are commonly used for temperature measurement. To create the thermoelectric effect, you need two different materials connected at opposite ends to make a closed circuit. These materials are usually semiconductors or conductive elements with different electrical properties. It is important to have a temperature difference between the two ends. One end gets heated, called the "hot end," while the other end is kept cold, known as the "cold end." This temperature difference causes electrons to move from the hot end to the cold end within the material. This movement of electrons generates an electric voltage that appears at the connection points. This voltage could be connected to an external circuit, allowing to produce electric power. Obviously, the greater the temperature difference, the higher amount of energy harvest (just like the PVT systems) (Zareie et al., 2024). This process is the foundation of how thermoelectric generators work. The Seebeck effect is highly significant because it enables the direct conversion of heat into electrical energy without the need for moving parts or combustion, making it an efficient and reliable method for various applications (Lee, 2016). While thermoelectric materials have been known for quite some time, ongoing research aims to develop more efficient and cost-effective materials for a wide range of practical applications, including waste heat recovery, power generation in space probes, and even thermoelectric cooling systems for consumer electronics (Chen et al., 2023; Sanad et al., 2020).

Several contributions have taken in this area. For instance, Liu et al. (Liu et al., 2015) studied the feasibility of using thermoelectric power generators to harness energy from an automotive exhaust pipe. They constructed an energy-harvesting system and developed a test bench to analyze its performance characteristics. Through road tests and revolving drum test table experiments, they designed a new system and integrated it into a prototype vehicle named "Warrior." The system's hot-side temperature, cold-side temperature, open circuit voltage, and power output were thoroughly examined, leading to the achievement of a maximum power output of 944 W, making it suitable for automotive applications. This study demonstrates the promising potential of utilizing thermoelectric generators for recovering low-temperature waste heat in vehicles. In another study, Meng et al. studied the development of a multiphysics thermoelectric generator model designed for the recovery of waste heat from automobile exhaust systems. This model incorporates a detailed representation of the exhaust heat source and the water-cooling heat sink. The research places particular emphasis on addressing the non-uniformity of temperature differences across thermoelectric units in the streamwise direction, as this non-uniformity can significantly impact the performance of exhaust thermoelectric generator systems. Kempf and Zhang (Kempf & Zhang, 2016) studied the potential for enhancing automotive fuel efficiency through the utilization of thermoelectric power generation, which harnesses exhaust waste heat. They conducted a simulation of a high-temperature thermoelectric generator applied to a light-duty passenger vehicle with a 4-cylinder gasoline engine. The research focuses on optimizing the thermoelectric generator configuration and heat exchanger design to achieve the maximum improvement in fuel efficiency. He et al. (He et al., 2016) studied the development of a comprehensive numerical model for thermoelectric generators applied to the recovery of exhaust waste heat from engines. This model is based on a common plate-type exhaust heat exchanger and takes into account various factors crucial for effective heat recovery. Kim et al. (He et al., 2016) introduced the concept of a Direct Contact Thermoelectric Generator (DCTEG) to enhance the practicality and expand the applications of thermoelectric generators. In a DCTEG, one surface of a thermoelectric module is in direct contact with a heat source, while the other surface is directly exposed to a coolant flow. This direct contact configuration simplifies system fabrication, maintenance, and improves long-term reliability, making it suitable for various applications in cooperation with other energy systems. It eliminates the need for interfaces between thermoelectric modules and heat sources.

While numerous studies have been carried out in this domain, the research deficiency stems from the lack of a simplified numerical model for thermoelectric systems in diesel engines and the absence of a thorough examination of the key factors that influence their operational efficiency. Such a model would facilitate the understanding and optimization of thermoelectric generators, promoting their application in waste heat recovery and energy efficiency improvements in diesel engine vehicles.

In this study, we used a straightforward model for assessing thermoelectric energy harvesting systems. Concurrently, finite element simulations were employed to assess this model. We conducted a comparative analysis of the outcomes from both approaches against experimental data from the literature to validate the model's accuracy. Additionally, we examined the system's performance across 12 distinct operational modes of the diesel engine at varying loads and speeds.

METHODOLOGY

In the present study, a numerical method is presented and implemented to investigate the thermoelectric performance under various motor loads and rotations.

The model is presented by assuming the following:

- Relationships are calculated in a steady state.
- The Seebeck coefficient does not depend on temperature.
- Heat transfer in each PN junction is one-dimensional.
- The heat and electricity resistance of the surfaces is neglected.
- Radiant heat transfer and displacement in the elements are neglected.
- PN links are placed in parallel.

The heat absorbed at the thermoelectric hot head is obtained from Equation (1) and the heat released at its cold head is obtained from Equation (2). The h and c subscripts are expressed in regards to the hot and cold heads of the thermocouples.

$$\dot{\boldsymbol{Q}}_{\boldsymbol{h}} = \boldsymbol{n}\left(\boldsymbol{\alpha T_h I} - \frac{\mathbf{1}}{\mathbf{2}}\boldsymbol{I^2 R} + \boldsymbol{k}(\boldsymbol{T_h} - \boldsymbol{T_c})\right) \tag{1}$$

$$\dot{\boldsymbol{Q}}_{\boldsymbol{c}} = \boldsymbol{n}\left(\boldsymbol{\alpha T_c I} + \frac{\mathbf{1}}{\mathbf{2}}\boldsymbol{I^2 R} + \boldsymbol{k}(\boldsymbol{T_h} - \boldsymbol{T_c})\right) \tag{2}$$

Where n denotes the number of thermocouples, T is the temperature, I represents the current, R denotes the resistance, k is the heat conduction coefficient, and α is the Seebeck coefficient. α, R, and k can be calculated by

$$\boldsymbol{\alpha} = \boldsymbol{\alpha_P} - \boldsymbol{\alpha_N} \tag{3}$$

$$\boldsymbol{R} = \frac{\boldsymbol{\rho_P l_P}}{\boldsymbol{A_P}} + \frac{\boldsymbol{\rho_N l_N}}{\boldsymbol{A_N}} \tag{4}$$

$$\boldsymbol{k} = \frac{\boldsymbol{k_P A_P}}{\boldsymbol{l_P}} + \frac{\boldsymbol{k_N A_N}}{\boldsymbol{l_N}} \tag{5}$$

Where l and A represent the length and cross-sectional area of the thermoelements and ρ denotes the density. The P and N subscripts are expressed in terms of the P-type and N-type thermoelements.

By applying the first law of thermodynamics in the thermoelectric module, the equation $\dot{W} = \dot{Q}_h - \dot{Q}_c$ is established. The output power of each module can be rewritten by subtraction of Equation (2) from Equation (1)

$$\dot{\boldsymbol{W}}_{\boldsymbol{n}} = \boldsymbol{n}(\boldsymbol{\alpha I}(\boldsymbol{T_h} - \boldsymbol{T_c}) - \boldsymbol{I^2 R}) \tag{6}$$

The power of the module can also be calculated according to the external load resistance, shown as

$$\dot{\boldsymbol{W}}_{\boldsymbol{n}} = \boldsymbol{n I^2 R_L} \tag{7}$$

The voltage value can also be calculated from Equation $\dot{W}_n = V_n I$. Equations (8) and (9) show the output voltage for each module.

$$\boldsymbol{V_n} = \boldsymbol{n}(\boldsymbol{\alpha}(\boldsymbol{T_h} - \boldsymbol{T_c}) - \boldsymbol{IR}) \tag{8}$$

$$\boldsymbol{V_n = nIR_L} \tag{9}$$

By equating Equations (8) and (9), the amount of electric current of the module is also obtained. The amount of electric current of the module is obtained from Equation (10).

$$\boldsymbol{I = \frac{\alpha(T_h - T_c)}{R_L + R}} \tag{10}$$

By replacing Equation (10) in Equations (7) and (9), the output voltage and power of each module can be obtained in terms of internal resistance and load. Equations (11) and (12) show the amount of voltage and output power of each module.

$$\boldsymbol{V_n = \frac{n\alpha R_L(T_h - T_c)}{R_L + R}} \tag{11}$$

$$\boldsymbol{\dot{W}_n = \frac{n\alpha^2 R_L(T_h - T_c)^2}{(R_L + R)^2}} \tag{12}$$

Validation

We validate the model implementation with experimental results presented by Kim et al. (Kim, Negash, et al., 2016). The thermoelectric generator is assumed to be connected to the exhaust gas channel of the diesel engine to harvest energy from the waste heat. In their research study, an investigation was conducted to assess the waste heat recovery capabilities of a thermoelectric generator under various operating conditions. Three distinct engine rotation cycles, namely 1000, 1500, and 2000 rpm, were selected as the primary variables of interest. Additionally, a range of motor loads spanning from 0.2 MPa to 0.1 MPa was examined. Consequently, a total of 12 distinct motor states, characterized by different combinations of rotation speeds and loads, were systematically explored. The work presented by Kim et al. (Kim, Lee, et al., 2016) comprehensively elucidated the thermoelectric generator's structure and provided equations governing the heat transfer processes within the exhaust system. This allowed for the determination of the inlet and outlet temperatures of the car's exhaust gas under various engine loads and rotation speeds. Notably, the thermoelectric cold head was actively cooled by a water stream maintained at 293 K, while the hot head was thermally coupled to the combustion gases originating from the engine's exhaust. The water flow rate was maintained at a constant 8 lit/min. To capture the variations in temperature, thermometers were strategically positioned at both the exhaust's inlet and outlet, enabling measurements under diverse engine conditions. Table 1 presents the values of the inlet and outlet gas temperatures in different engine states, presented by (Kim, Lee, et al., 2016).

Table 1 Inlet and outlet temperature of exhaust gas at different engine speeds and loads (Kim, Lee, et al., 2016).

RPM / MPa	1000		1500		2000	
	outlet	inlet	outlet	inlet	outlet	inlet
0.2	358	413	383	446	424	489
0.4	391	473	424	511	474	550
0.6	432	529	462	561	512	599
0.8	462	572	500	607		
1.0	494	625				

The thermoelectric material used is bismuth telluride (Bi_2Te_3) and its Seebeck coefficient is 400 mV/K. The internal resistance of each module is also mentioned as 2 Ω. Also, there are 40 modules of thermoelectric, so the power should be multiplied by 40 (Kim, Lee, et al., 2016; Lee, 2016).

The efficiency of the system can be calculated by

$$\eta = \frac{\dot{W}_n}{\dot{m}c_P(T_{in} - T_{out})} \tag{13}$$

Where c_P is the specific heat of charge in the exhaust, which is equal to 1030 J/(kgK) and $\dot{m}$ is the exhaust gas flow rate obtained in Table 2.

Table 2 Exhaust gas flow rate at different engine speeds and loads (kilogram per hour)

RPM MPa	1000	1500	2000
0.2	66	80	122
0.4	70	94	150
0.6	76	109	178
0.8	84	127	
1.0	92		

All the represented 12 conditions are analyzed with the presented model as well as the finite element method simulations. The results are compared with those presented by (Kim, Negash, et al., 2016).

RESULTS AND FINDINGS

Finite element method

This section of the research article delves into finite element simulations, focusing on the analysis of a single thermoelement within the PN (thermoelectric power generation module) with specific dimensions measuring 0.4×1.4×1.4 mm. The simulations are aimed at quantifying the thermoelement's output power. Subsequently, the calculated power output is scaled by a factor of 161 to represent the power output of an entire thermoelectric module, given the presence of 161 PNs within it. It is essential to note that, in this study, a configuration of 40 such modules is employed in a parallel arrangement to enhance overall performance. Additionally, to account for experimental uncertainties, a correction factor of 1.35 is applied to the power calculations.

Within this context, the resistance used to harvest energy remains constant at 2 Ω. However, the section investigates the impact of varying pressures on the thermoelectric hot part's temperature, considering that the cold part maintains a constant temperature of 293 K. The temperature of the PN junction's hot part aligns with the average inlet and outlet temperatures of the exhaust system. Figure (1–3) graphically illustrates the temperature distribution of both the hot and cold sections, along with the maximum achievable output power, across a pressure range spanning from 0.2 to 1 MPa under engine speeds of 1000, 1500, and 2000 rpm.

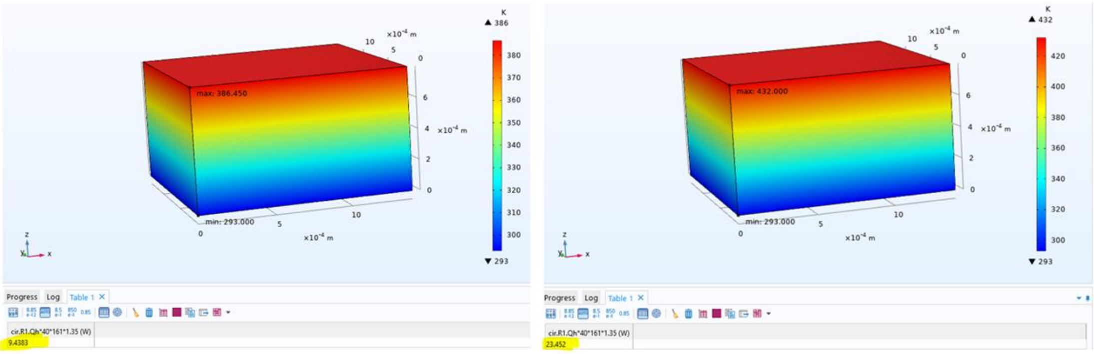

cir.R1.Qh*40*161*1.35 (W)
9.4383

cir.R1.Qh*40*161*1.35 (W)
23.452

(a) 0.2 MPa motor load

(b) 0.4 MPa motor load

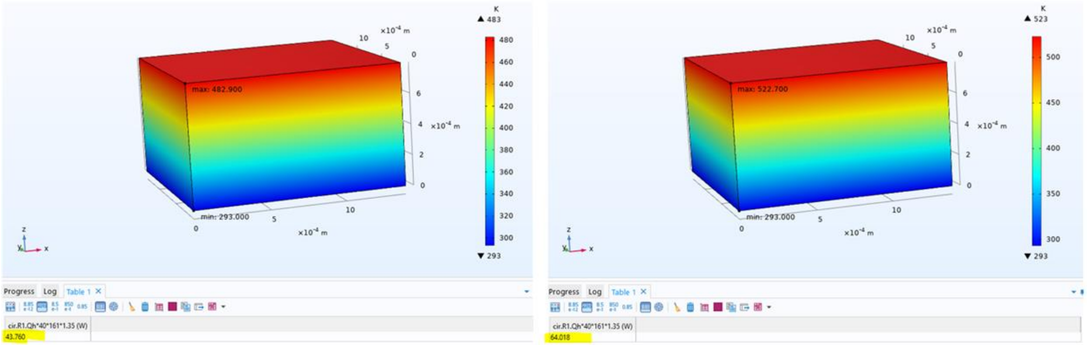

cir.R1.Qh*40*161*1.35 (W)
43.760

cir.R1.Qh*40*161*1.35 (W)
64.018

(c) 0.6 MPa motor load

(d) 0.8 MPa motor load

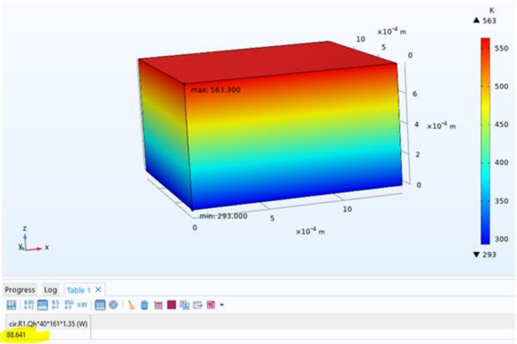

cir.R1.Qh*40*161*1.35 (W)
88.641

(e) 1.0 MPa motor load

Figure 1 Temperature contour of a single thermoelement and total harvested power in 1000 rpm.

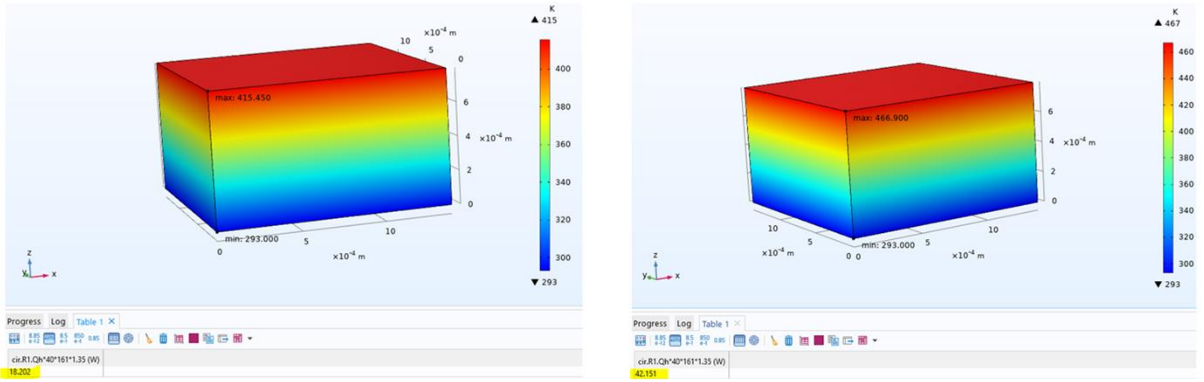

cir.R1.Qh*40*161*1.35 (W)
18.202

cir.R1.Qh*40*161*1.35 (W)
42.151

(a) 0.2 MPa motor load **(b) 0.4 MPa motor load**

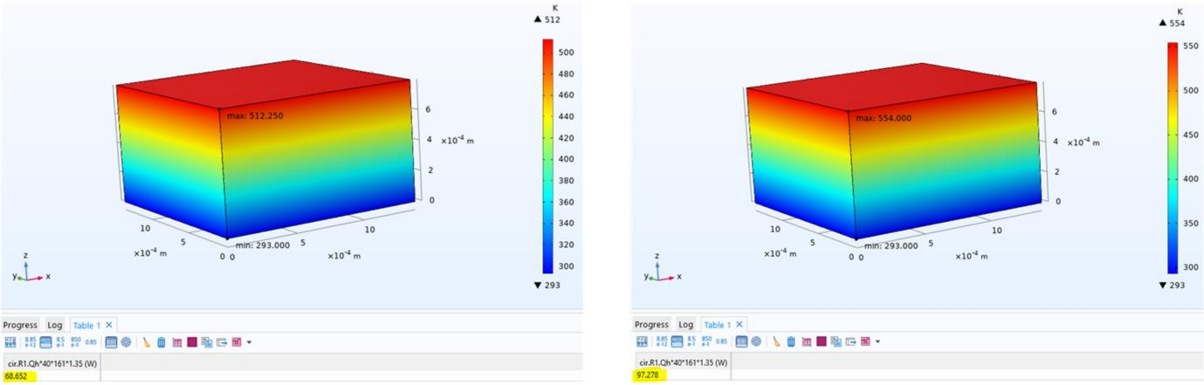

cir.R1.Qh*40*161*1.35 (W)
68.652

cir.R1.Qh*40*161*1.35 (W)
97.278

(c) 0.6 MPa motor load **(d) 0.8 MPa motor load**

Figure 2 Temperature contour of a single thermoelement and total harvested power in 1500 rpm.

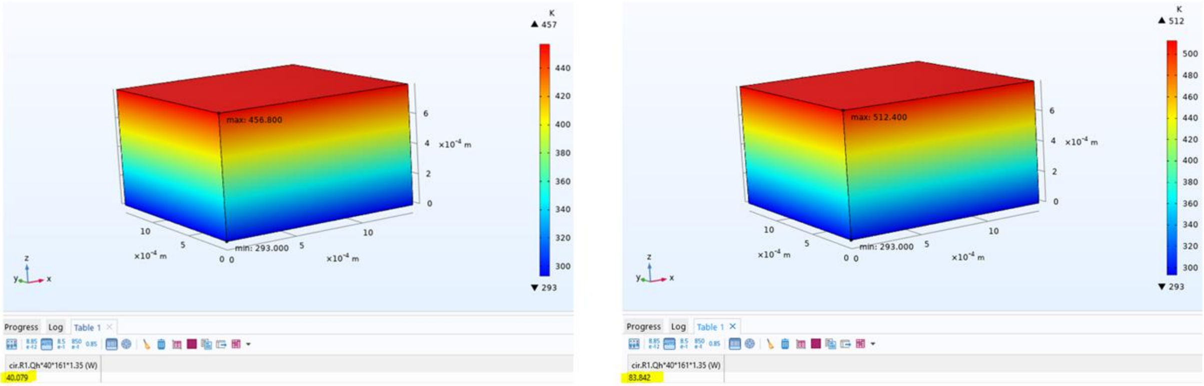

cir.R1.Qh*40*161*1.35 (W)
40.079

cir.R1.Qh*40*161*1.35 (W)
83.842

(a) 0.2 MPa motor load **(b) 0.4 MPa motor load**

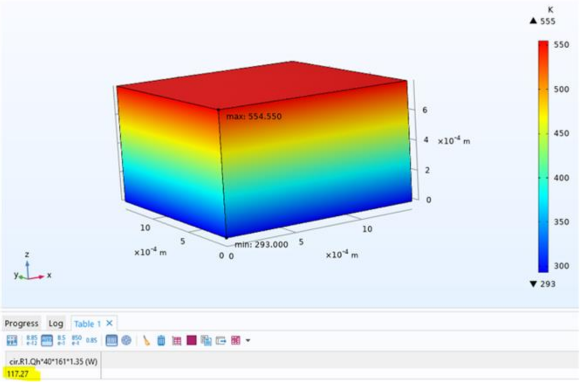

cir.R1.Qh*40*161*1.35 (W)
117.27

(c) 0.6 MPa motor load

Figure 3 Temperature contour of a single thermoelement and total harvested power in 2000 rpm.

Numerical model

The results related to the numerical calculations section have been performed in MATLAB software. Figure (4) shows the amount of power taken from the thermoelectric generating system at 1000 rpm as a function of load resistance. Figure (5) shows the amount of power taken from the thermoelectric generating system at 1500 rpm as a function of load resistance. Figure (6) shows the amount of power taken from the thermoelectric generating system at 2000 rpm as a function of load resistance. As expected, with the increase in engine speed and load, as the exhaust temperature increases, the temperature of the hot head increases and the temperature of the cold head remains constant, which leads to more electricity production. Figure (7) shows the efficiency of the system. In the cases that are investigated, the efficiency is also increased with the rise in load and engine speed.

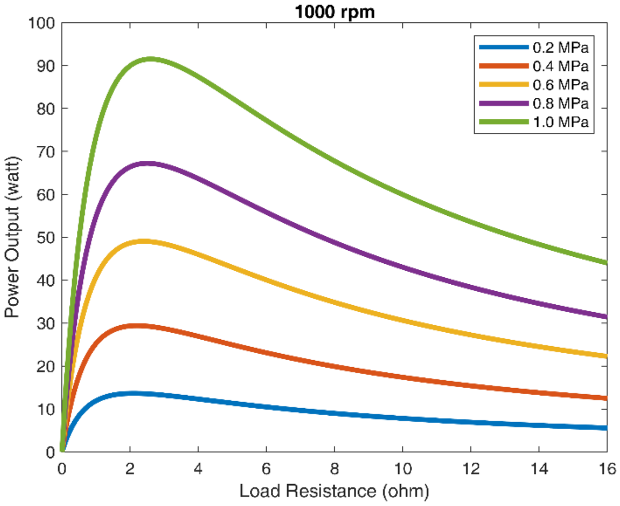

Figure 1 The amount of power taken from the thermoelectric generating system at 1000 rpm as a function of load resistance

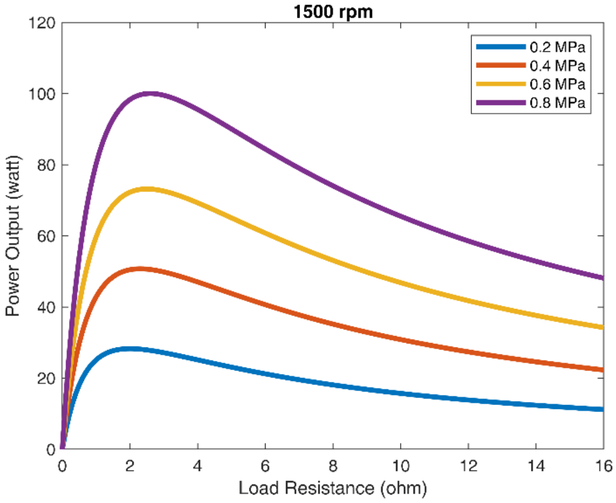

Figure 2 The amount of power taken from the thermoelectric generator system at 1500 rpm as a function of load resistance

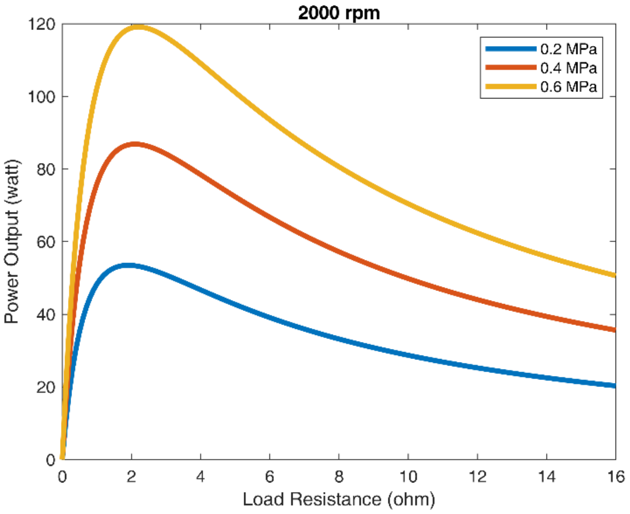

Figure 3 Power output from a thermoelectric generator system at 2000 rpm as a function of load resistance

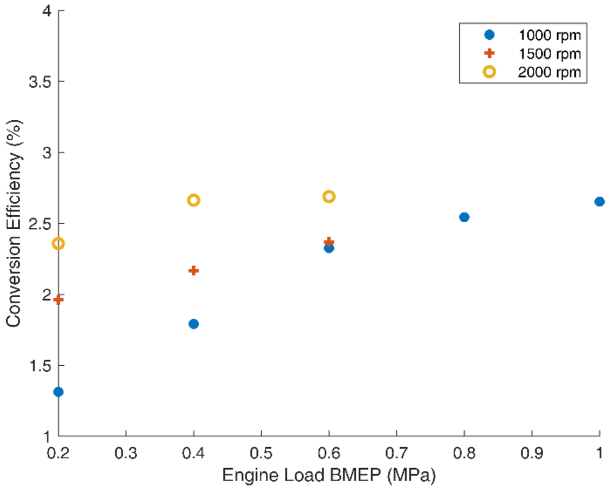

Figure 4 System efficiency at various motor velocities.

Verification

In Table 3, the values obtained by finite element method and numerical method are compared with the values presented by (Kim, Negash, et al., 2016). This comparison indicates an acceptable.

Table 3 Comparison between results of experimental, finite element method, and numerical methods.

	Maximum output power (W)				Relative error (%)	
Velocity (rpm)	**Load (MPa)**	**Experiments (Kim, Negash, et al., 2016)**	**Numerical model**	**Finite element simulation**	**Numerical model**	**Finite element simulation**
1000	**0.2**	9.5	12	9.4	1%	28%
	0.4	24	29	23.4	3%	24%
	0.6	44.9	48	43.8	3%	10%

	0.8	67.3	67	64	5%	5%
	1.0	91.5	92	88.6	3%	4%
1500	**0.2**	19.2	24	18.2	5%	32%
	0.4	43.9	50	42.1	4%	19%
	0.6	71	74	68.6	3%	8%
	0.8	100	100	97.3	3%	3%
2000	**0.2**	44.1	53	40.1	10%	32%
	0.4	86.1	84	83.8	3%	0%
	0.6	119.1	119	117.3	2%	1%

CONCLUSION

In conclusion, this study underscores the significant potential of thermoelectric generators in addressing the growing global energy demands and environmental imperatives. The utilization of waste heat sources, notably exhaust emissions from internal combustion engines, offers a pivotal pathway to enhance energy efficiency and mitigate emissions. The research introduced a comprehensive model for assessing thermoelectric generator performance in the context of recovering heat from diesel engine exhaust. By situating 14 thermoelectric modules within the gas channel of the engine, with the hot side exposed to exhaust gas and the cold side cooled by water at a fixed temperature of 293 K, the study explored 12 distinct engine operating modes. These encompassed three motor speed settings (1000, 1500, and 2000 rpm) and five motor load conditions (ranging from 0.2 to 1.0 MPa). Notably, this investigation combined numerical analysis with finite element simulations, with the results demonstrating a strong alignment between numerical and experimental findings. In sum, this research underscores the promise of thermoelectric technology as a valuable contributor to sustainable energy solutions in the context of heat recovery from diesel engine exhaust.

REFERENCES

Asadi, M., Ahmadi, R., & Abazari, A. M. (2023). Footstep-Powered Floor Tile: Design and Evaluation of an Electromagnetic Frequency Up-Converted Energy Harvesting System Enhanced by a Cylindrical Halbach Array. *Sustainable Energy Technologies and Assessments*.

Asadi, M., Larki, I., Forootan, M. M., Ahmadi, R., & Farajollahi, M. (2023). Long-Term Scenario Analysis of Electricity Supply and Demand in Iran: Time Series Analysis, Renewable Electricity Development, Energy Efficiency and Conservation. *Sustainability*, *15*(5), 4618. https://doi.org/10.3390/su15054618

Chen, K., Wang, L., Luo, Z., Xu, X., Li, Y., Liu, S., & Zhao, Q. (2023). Flexible Thermoelectrics Based on Plastic Inorganic Semiconductors. *Advanced Materials Technologies*, *8*(16). https://doi.org/10.1002/admt.202300189

He, W., Wang, S., Li, Y., & Zhao, Y. (2016). Structural size optimization on an exhaust exchanger based on the fluid heat transfer and flow resistance characteristics applied to an automotive thermoelectric generator. *Energy Conversion and Management*, *129*, 240–249. https://doi.org/10.1016/j.enconman.2016.10.032

Kempf, N., & Zhang, Y. (2016). Design and optimization of automotive thermoelectric generators for maximum fuel efficiency improvement. *Energy Conversion and Management*, *121*, 224–231. https://doi.org/10.1016/j.enconman.2016.05.035

Kim, T. Y., Lee, S., & Lee, J. (2016). Fabrication of thermoelectric modules and heat transfer analysis on internal plate fin structures of a thermoelectric generator. *Energy Conversion and Management*, *124*, 470–479. https://doi.org/10.1016/j.enconman.2016.07.040

Kim, T. Y., Negash, A. A., & Cho, G. (2016). Waste heat recovery of a diesel engine using a thermoelectric generator equipped with customized thermoelectric modules. *Energy Conversion and Management*, *124*, 280–286. https://doi.org/10.1016/j.enconman.2016.07.013

Larki, I., Zahedi, A., Asadi, M., Forootan, M. M., Farajollahi, M., Ahmadi, R., & Ahmadi, A. (2023). Mitigation approaches and techniques for combustion power plants flue gas emissions: A comprehensive review. *Science of The Total Environment*, *903*, 166108. https://doi.org/10.1016/j.scitotenv.2023.166108

Lee, H. (2016). *Thermoelectrics: design and materials*. John Wiley & Sons.

Liu, X., Deng, Y. D., Li, Z., & Su, C. Q. (2015). Performance analysis of a waste heat recovery thermoelectric generation system for automotive application. *Energy Conversion and Management*, *90*, 121–127. https://doi.org/10.1016/j.enconman.2014.11.015

Sanad, M. F., Shalan, A. E., Abdellatif, S. O., Serea, E. S. A., Adly, M. S., & Ahsan, M. A. (2020). Thermoelectric Energy Harvesters: A Review of Recent Developments in Materials and Devices for Different Potential Applications. *Topics in Current Chemistry*, *378*(6), 48. https://doi.org/10.1007/s41061-020-00310-w

Zareie, Z., Ahmadi, R., & Asadi, M. (2024). A comprehensive numerical investigation of a branch-inspired channel in roll-bond type PVT system using design of experiments approach. *Energy*, *286*, 129452. https://doi.org/10.1016/j.energy.2023.129452